

Modelling maize phenology, biomass growth and yield under contrasting temperature conditions

Na Wang^{a,b}, Enli Wang^{b,*}, Jing Wang^{a,*}, Jianping Zhang^c, Bangyou Zheng^d, Yi Huang^a, Meixiu Tan^a

^a College of Resources and Environmental Sciences, China Agricultural University, Beijing 100193, China

^b CSIRO Agriculture and Food, GPO Box 1700, Canberra ACT 2601, Australia

^c Chongqing Institute of Meteorological Sciences, Chongqing 401147, China

^d CSIRO Agriculture and Food, Queensland Biosciences Precinct, 306 Carmody Road, St. Lucia 4067, Australia

ARTICLE INFO

Keywords:

Temperature responses
Leaf growth
Phasic development
Radiation use efficiency
APSIM
Climate warming

ABSTRACT

Crop modelling has become an effective means to assess climate change impact on crop yield and to assist in development of adaptation strategies. Previous studies found large uncertainty in simulated crop yields, especially beyond optimal temperature range. In this paper, we combined the data reported in literature and our controlled-temperature experiment to derive the temperature response functions of phenological development and biomass growth of maize crop based on the Wang-Engel function (*Agricultural systems*, 58(1): 1–24), and compared them with those adopted in two mostly used maize growth models APSIM-Maize and CERES-Maize. Our results support the previous findings that leaf elongation, leaf appearance and the rate of development towards flowering have the same temperature response. Our results indicate that a curvilinear response with cardinal temperatures of 5 °C (base), 30 °C (optimum), and 41 °C (maximum) best describes the maize developmental response to temperature. For radiation use efficiency (RUE-biomass growth per unit intercepted radiation) of maize, the corresponding cardinal temperatures are likely to be 2 °C, 24 °C, and 38 °C respectively. All the cardinal temperatures are lower than what are used in current APSIM model. Replacing the default temperature responses with the newly derived ones led to contrasting differences in simulated flowering and maturity time across China's Maize Belt, while the differences in simulated maize yield were relatively smaller. This implies the importance to use the correct temperature response in maize growth modelling so that the genotype by environment interactions in response to rising temperature can be correctly captured.

1. Introduction

Extreme high temperature events occurred more frequently in the past decades and are projected to increase in magnitude, duration, and frequency (IPCC, 2012). Climate warming has had significant impacts on agricultural productions (Lobell et al., 2011, 2013; Piao et al., 2010; Wang et al., 2011). Accurately assessing the impacts of climate warming on crop yield is essential in developing effective adaptation strategies for agriculture adapting to climate change (IPCC, 2014; Parry et al., 2004; Rosenzweig and Wilbanks, 2010).

Maize is one of the most important grain crops, and has the largest total production (FAO, 2014). Maize production in China accounts for 17% of global total (Xiong et al., 2009). Previous studies showed that high temperature would lead to the decrease in maize growth period (Badu et al., 1983; Hunter et al., 1977; Warrington and Kanemasu, 1983) and final yield (Badu et al., 1983; Kiesselbach, 1950; Siebert

et al., 2014). Accurate assessment of the impact of high temperature on maize growth and development could help develop appropriate options to ensure China's and global security of maize production (Tao and Zhang, 2010). Such assessment will require reliable predictions of maize yield in response to rising temperature.

Crop models have been recognized effective tools to evaluate the impacts of future climate change on crop production (Bassu et al., 2014). However, large uncertainties exist in simulated crop yield, particularly in response to rising temperature beyond the optimal range, which is the key finding of multi-model inter-comparison studies for wheat (Asseng et al., 2013), maize (Bassu et al., 2014), rice (Li et al., 2015), and potato (Fleisher et al., 2017). A more recent study by Wang et al. (2017) demonstrates that inaccuracies in temperature response functions of the key processes simulated in the wheat models explained more than 50% of the uncertainty in simulated wheat yield, and that improved temperature functions based on data could reduce the

* Corresponding authors.

E-mail addresses: Enli.Wang@csiro.au (E. Wang), wangj@cau.edu.cn (J. Wang).

<https://doi.org/10.1016/j.agrformet.2018.01.005>

Received 8 September 2017; Received in revised form 27 December 2017; Accepted 2 January 2018

Available online 11 January 2018

0168-1923/ © 2018 Elsevier B.V. All rights reserved.

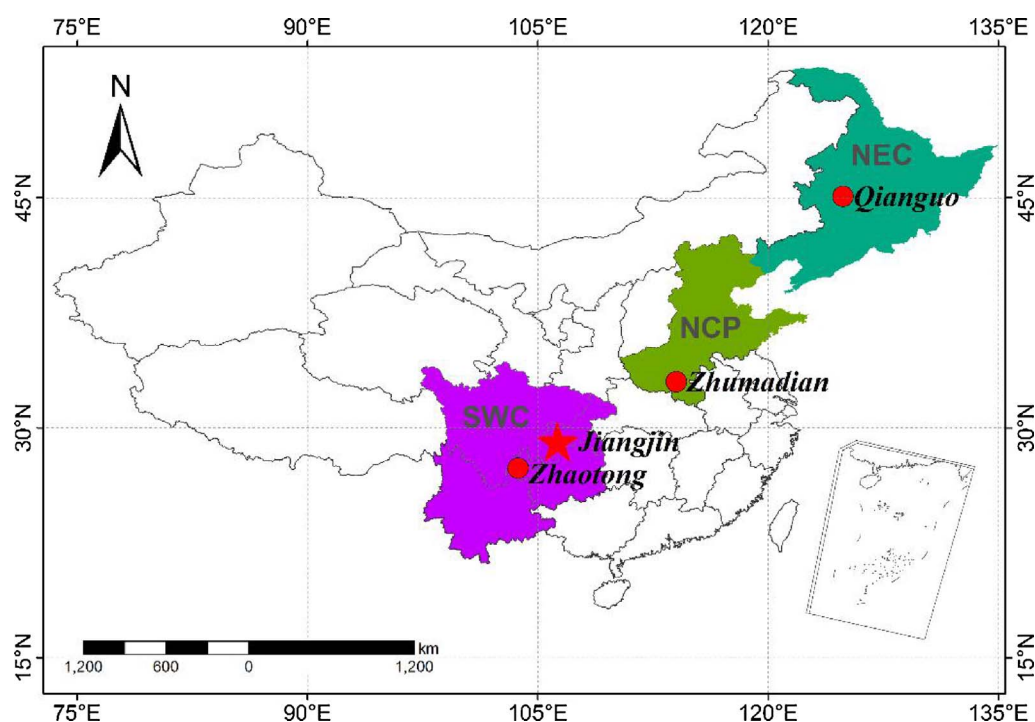


Fig. 1. The geographic locations of Northeast China (NEC), North China Plain (NCP), Southwest China (SWC) and the three study sites (Qianguo, Zhumadian, Zhaotong). The controlled-temperature experiment was conducted at Jiangjin agrometeorological experimental station in Southwest China.

Table 1

Site information, maize cultivars and growing periods at three study sites. NEC = Northeast China, NCP = North China Plain, SWC = Southwest China.

| Area | Site name | Latitude (°N) | Longitude (°E) | Altitude (m) | Growing season average temperature (°C) | Cultivar | Periods |
|------|-----------|---------------|----------------|--------------|---|--------------|---|
| NEC | Qianguo | 45.08 | 124.87 | 136.2 | 19.8 | Jidan_180 | 2007–2009 (calibration) 2010–2011 (validation) |
| NCP | Zhumadian | 33.00 | 114.02 | 82.7 | 25.2 | Zhengdan_958 | 2004–2006 (calibration) 2007–2009 (validation) |
| SWC | Zhaotong | 27.35 | 103.72 | 1949.5 | 18.5 | Tongdan_2 | 1994–1997 (calibration) 1998–2001 (validation) |

Table 2

Temperature, photoperiod, relative humidity and CO₂ concentration maintained in the phytotron during the controlled experiment.

| Temperature (°C) | | | Photoperiod (h) | Relative humidity (%) | CO ₂ concentration (ppm) |
|------------------|-------|------|-----------------|-----------------------|-------------------------------------|
| Day | Night | Mean | | | |
| 25 | 15 | 20 | 13 | 65 | 450 |
| 35 | 25 | 30 | | | |
| 35 | 35 | 35 | | | |
| 40 | 35 | 37.5 | | | |

simulation error by up to 50%. For maize, similar issues may also exist because response functions in current maize models may have been developed with the data from limited controlled-temperature and field experiments under a narrow range of temperatures (Brown and Bootsma, 1993; Gilmore and Rogers, 1958; Stewart et al., 1998; Yan and Hunt, 1999; Yin et al., 1995).

Parent and Tardieu (2012) found the Arrhenius-type curve could describe the response of crop development to a large range of temperature based on reviewing previous experimental data from the controlled-temperature and field experiments with contrasting climate conditions. However, the base and maximum temperatures for maize development could not be derived from Arrhenius-type curve. Parent and Tardieu (2014) further indicated that there may be a large uncertainty in the response function of radiation use efficiency (RUE) to temperature used in crop models. Such uncertainties warrant further work on temperature response of development, biomass growth and

yield of maize crop.

The objectives of this study are to: (1) compare the temperature response functions for maize phenological development and biomass growth derived from data and those used in two maize crop models, i.e., APSIM and CERES, (2) derive new temperature response functions based on newest data and understanding, and (3) use APSIM model to investigate the impact of changed temperature response functions on simulated maize yield across contrasting maize growing regions of China under climate warming scenarios.

2. Materials and methods

2.1. Study sites

Three sites are selected in this study, including Qianguo in Northeast China (NEC), Zhumadian in North China Plain (NCP) and Zhaotong in Southwest China (SWC), where long-term maize data from an agrometeorological station at each site are available. The three sites cover the major climate types in China's Maize Belt (Fig. 1 and Table 1). Northeast China has a temperate monsoon climate where spring maize is sown on in early May and harvested in late September in a single-cropping system (one crop a year). The North China Plain is characterised by temperate humid/semi-humid climate where summer maize is sown in mid-June and harvested in late September in a winter wheat and summer maize double cropping system (two crops a year). Southwest China has a mixed subtropical and alpine frigid climate where maize is sown in early March to early May and harvest in late July to late September in a mixture of single-cropping system and

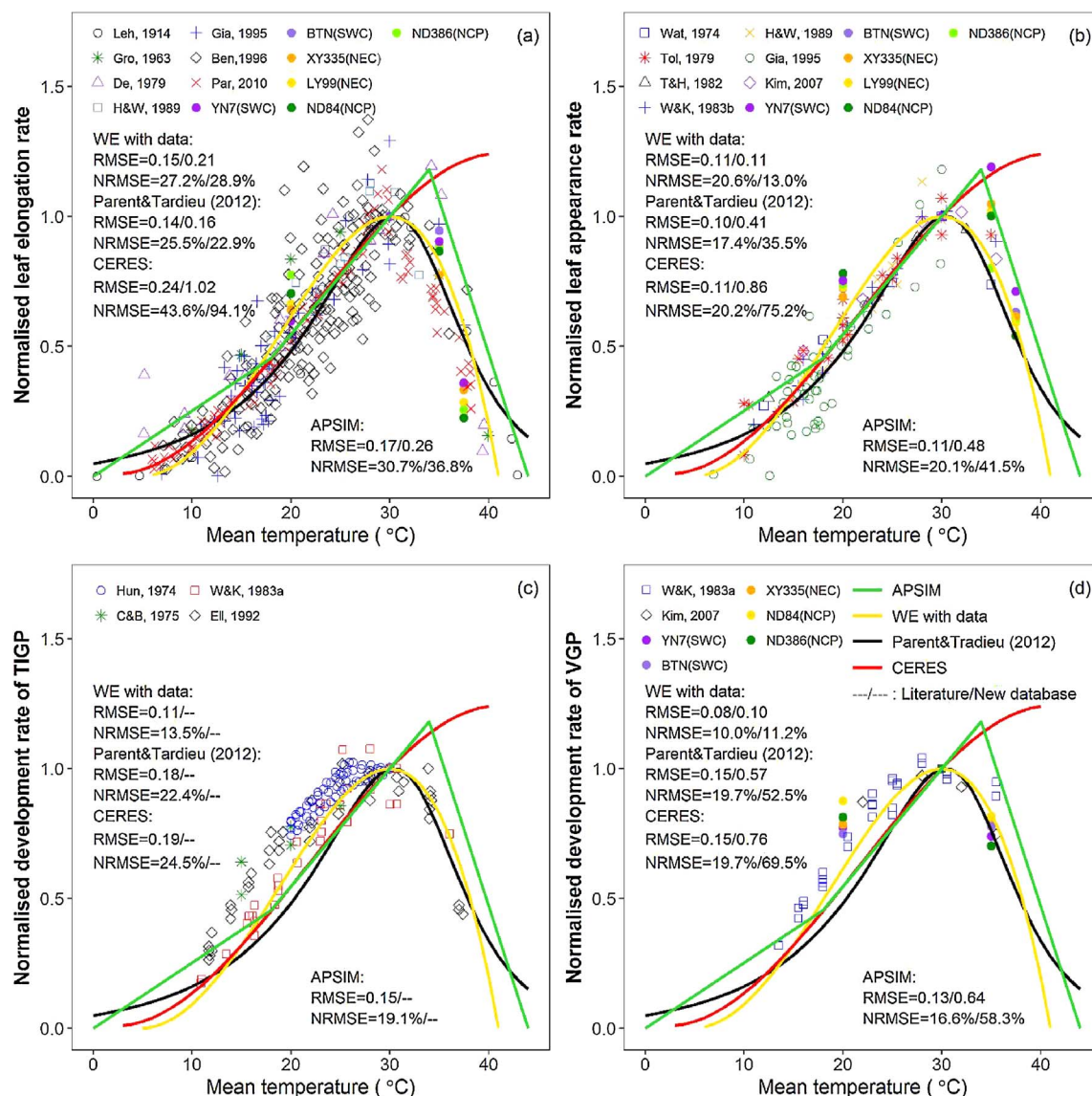


Fig. 2. Comparisons of the response of leaf elongation rate (LER) (a), leaf appearance rate (LAR) (b), development rate from emergence to tassels initiation (c) and development rate from emergence to anthesis/silking (d) to temperature. Curves are what used in APSIM & CERES models, the Arrhenius-curve derived by Parent and Tardieu (2012), and our fitted Wang-Engel function (WE). All the symbols denote data either from the literatures or from our controlled-temperature experiment. RMSE and NRMSE values at each panel denote statistical data from the literatures and controlled-temperature experiment, respectively.

double-cropping system. Detailed site information, prevailing maize cultivars and growth periods are summarised in Table 1. Soil data for each site, including the soil bulk density, saturation water content, drained upper limit, permanent wilting point, soil texture and soil organic carbon content, are obtained from China Soil Scientific Database (<http://www.soil.csdb.cn/>).

2.2. Crop data

We combined observational data from field experiments conducted at the three agrometeorological stations, controlled-temperature environments at Jiangjin, and literature review to investigate the responses of phenological development and biomass growth of maize crop to a large range of temperature. Response of biomass growth was investigated in terms of radiation use efficiency (RUE), i.e., biomass growth per unit intercepted radiation.

2.2.1. Field experimental data

Long-term records (1981–2010) of key phenological stages, biomass

and grain yield of maize are available from the three agrometeorological stations. The typical cultivar with observational data for at least five years was selected at each site (Table 1). Observed phenological stages include time of sowing, emergence, flowering and maturity. Daily weather data, including daily mean, maximum and minimum temperatures (°C), rainfall (mm), sunshine hours (h), and relative humidity (%) are also available from China Meteorological Administration (Liu et al., 2012). These data are used to calibrate and validate original and modified APSIM models with different temperature response functions of maize growth and development.

2.2.2. Controlled-temperature experiment

An ancillary controlled-temperature experiment was conducted in a phytotron at Jiangjin agrometeorological experimental station, Chongqing city, China (Fig. 1) to investigate the impact of high-temperature on leaf growth and development of different maize cultivars from China's Maize Belt. Four temperature treatments were used with the photoperiod, relative humidity and CO₂ concentration in the phytotron kept constant (Table 2). Two temperature and humidity sensors

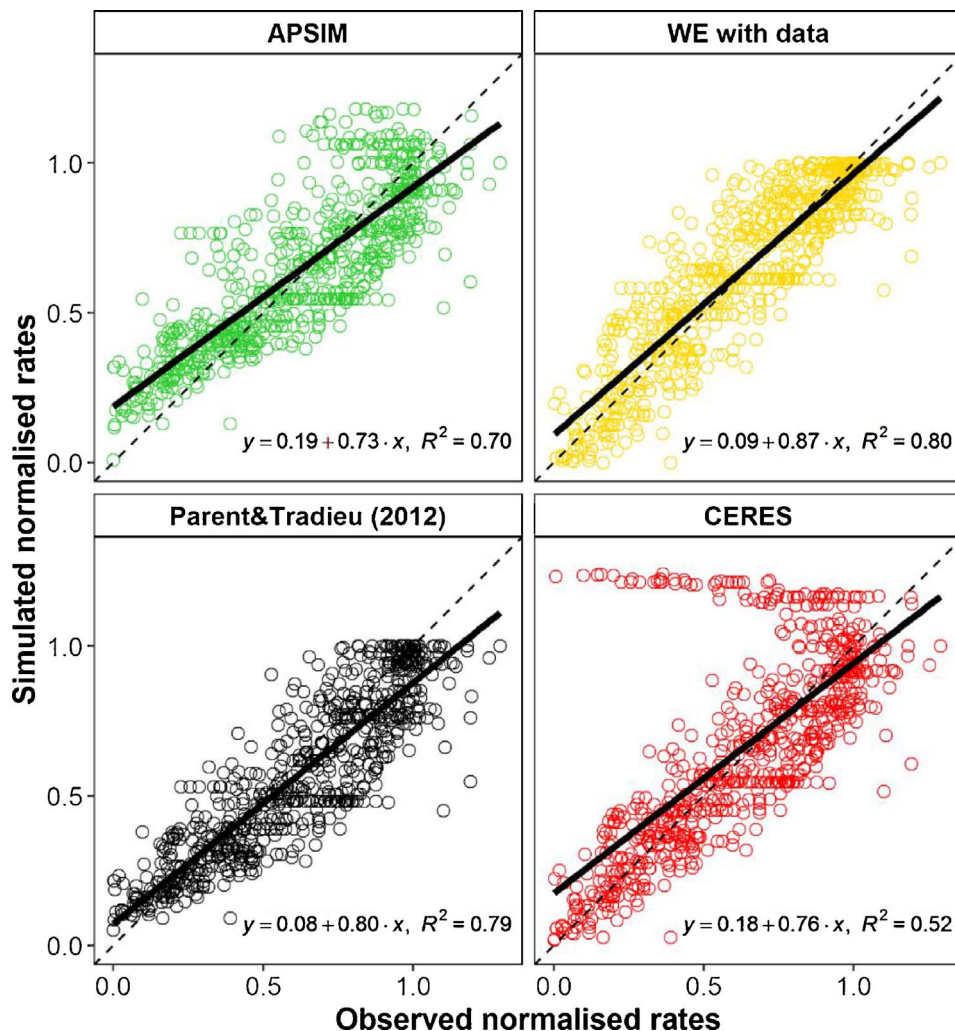


Fig. 3. Comparison of simulated and observed leaf growth and phenological development rates by APSIM, CERES, Arrhenius-curve of Parent and Tardieu (2012) and Wang-Engel function (WE). The dashed and solid lines were 1:1 line and linear regression line, respectively.

(Rotronic HF320) were mounted, each in the front and back of the phytotron, to monitor air temperature and relative humidity. The temperature change from day to night and night to day were programmed to occur over 30 min. Six 400 W metal halide lamps (blue light source) and sodium lamps (red light source) evenly distributed in each phytotron provided the necessary lights ($\sim 800 \mu\text{mol m}^{-2} \text{s}^{-1}$) for growing maize plants.

Six maize cultivars were selected, including representative cultivars 'Xianyu_335' and 'Liangyu_99' from Northeast China, 'Nongda_84' and 'Nongda_386' from North China Plain, 'Yunuo_7' and 'Baitiannuo' from Southwest China. Seed was sown (50 mm deep) in a growing medium of peat soil contained in 28-L pots. Two seeds were sown per pot and were then thinned to one seedling at the third-leaf stage. Four randomly arranged blocks were used for each cultivar within each treatment. Each plot was irrigated daily with about 400 ml of water to avoid any water stress. Compound fertilizer with N content of 24%, P_2O_5 content of 6% and K_2O content of 10% was applied twice before sowing and the third-leaf stages respectively with the same amount 20 g/pot and no nutrition stress was observed during the entire experiment period.

Leaf number, width and length of each leaf and maize phenological stages were recorded every day in each phytotron. Seedling emergence date was recorded when coleoptiles emerged from the soil. Leaf appearance was recorded when a leaf emerged 2 cm from the whorl. Leaf appearance rate (LAR, leaves/d) was estimated as the total number of leaves divided by the number of days elapsed. Leaf elongation rate (LER, cm/d) was calculated as the slope of linear regression between daily leaf length and the days after sowing until leaf full expansion. The

first five leaves originate from the embryo and the leaves after the fourteenth leaf grow normally faster. Therefore leaves from the sixth to the fourteenth were selected to investigate the response of leaf growth and development to temperature. These observed data in the phytotron are combined with data from literature to derive temperature response functions of maize development and growth.

2.2.3. Data extracted from literature review

We conducted a literature review of data describing temperature responses of key maize physiological processes, including leaf appearance, leaf elongation, phasic development rate (emergence to tasselling initiation, emergence to flowering or silking) and biomass growth in terms of radiation use efficiency (RUE), measured under either field or controlled-temperature environments (Supplementary Table S1). The WebPlotDigitizer software was used to extract the data from the published figures in the literatures (<http://arohatgi.info/WebPlotDigitizer/>).

Parent and Tardieu (2012) reviewed the temperature responses of tissue expansion, cell division and progression in plant cycle, and found that all these processes follow a common Arrhenius-type curve. For maize, the optimal temperature for those processes are around 30°C . However, different maize models used contrasting temperature response functions for phenological development as compared by Wang et al. (2015).

For temperature responses of biomass growth in terms of radiation use efficiency (RUE), there are very limited measurement data available (Supplementary Table S1). We tried to compare the limited data with

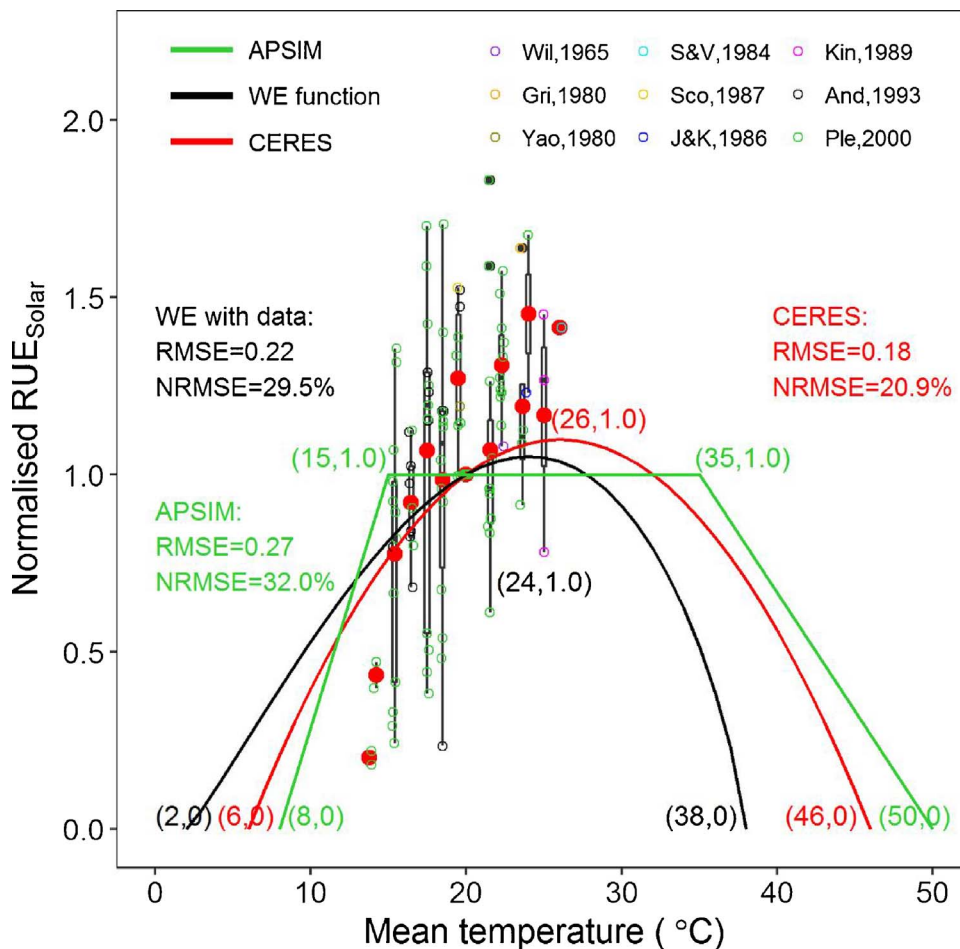


Fig. 4. Comparison of the response of maize RUE to temperature used in APSIM, CERES, and the new curve derived with Wang-Engel function (WE function).

Table 3
Cultivar parameters of three maize cultivars for original and modified APSIM.

| Parameter | Jidan_180 | | Zhengdan_958 | | Tongdan_2 | |
|---|-----------|----------|--------------|----------|-----------|----------|
| | Original | Modified | Original | Modified | Original | Modified |
| tt_emerg_to_endjuv (thermal time from emergence to the end of the juvenile period) | 130 | 182 | 210 | 310 | 280 | 280 |
| tt_flower_to_maturity (Thermal time from flower to the maturity (°Cd)) | 880 | 1000 | 810 | 930 | 750 | 850 |
| head_grain_no_max (maximum grain numbers per head) | 1000 | 750 | 500 | 550 | 700 | 700 |
| grain_gth_rate (grain-filling rate (mg/grain/day)) | 15 | 17 | 9.17 | 9.17 | 16 | 16 |
| tt_flower_to_start_grain (thermal time required from flowering to starting grain-filling (°Cd)) | 150 | 150 | 150 | 220 | 150 | 160 |

what are implemented in the two widely used maize growth models APSIM-Maize (Keating et al., 2003) and CERES-Maize (Jones and Kiniry, 1986). However, the limited temperature range and the large variations in observed data still led to large uncertainty in RUE response to temperature, especially above the optimum temperature. Wang et al. (2017) derived RUE response to temperature based on photosynthesis and respiration processes using Wang-Engel (WE) function for wheat. In this study, we also derived the temperature response function for maize RUE assuming that the photosynthesis temperature response and respiration has the same cardinal temperatures as reported in Wang et al. (2017).

2.3. Temperature response functions of maize growth and development

We used the Wang-Engel function (Wang and Engel, 1998, 2000) to derive the temperature response function for phenological development and RUE of maize respectively based on observed data. The function

simulates a curvilinear response based on three cardinal temperature, e.g. the base temperature (T_b), the optimum temperature (T_o) and the maximum temperature (T_x) of the simulated process, and gives a value of 0–1 between T_b and T_x . An extra shape factor β was added here in Eq. (1) to account for temperature responses with more extended T_o for RUE:

$$f(T) = \left(\frac{2(T - T_b)^\alpha (T_o - T_b)^\alpha - (T - T_b)^{2\alpha}}{(T_o - T_b)^{2\alpha}} \right)^\beta, \\ \alpha = \frac{2}{\ln\left(\frac{T_x - T_b}{T_o - T_b}\right)}, \\ \beta = 0 \sim 1 \quad (1)$$

The derived temperature response functions were then compared with Arrhenius-type curve and what was used in both APSIM- and CERES- Maize models.

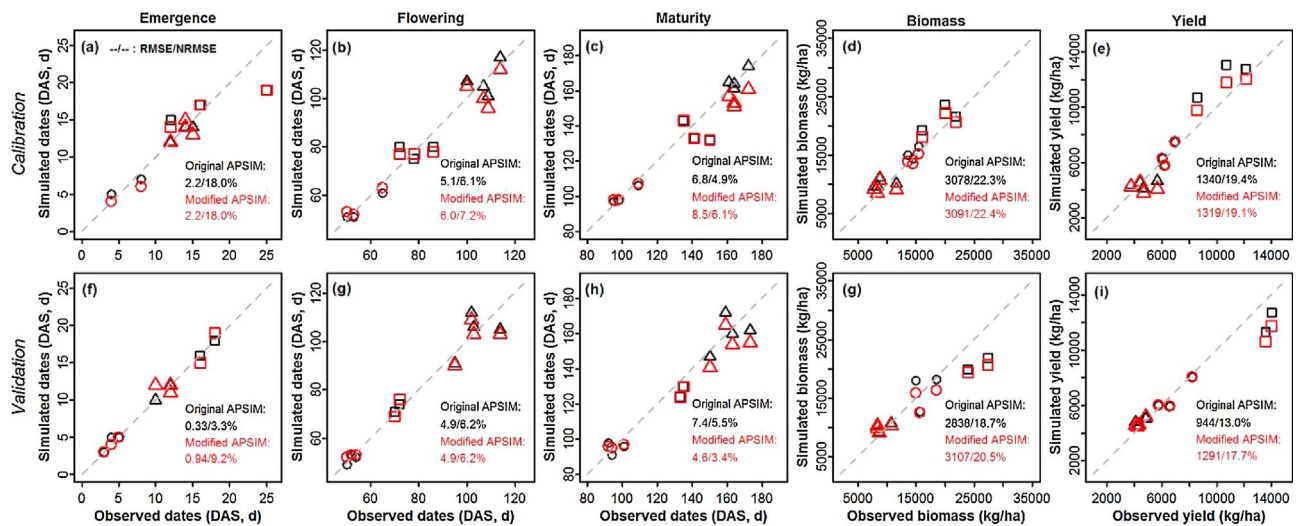


Fig. 5. Comparison of simulated and observed emergence date (days after sowing, DAS) (a and f), flowering date (DAS, b and g), maturity date (DAS, c and h), biomass (kg/ha, d and g) and grain yield (kg/ha, e and i) for original and modified APSIM. (a–f) Model calibration, (g–i) model validation. The dashed line shows 1:1 line. The black points represent original APSIM and red points represent modified APSIM. The points with different shapes represent different maize cultivars. Square represents Jidan_180 used in Northeast China, circle represents Zhengdan_958 used in North China Plain and triangle represents Tongdan_2 used in Southwest China. (For interpretation of the references to colour in this figure legend, the reader is referred to the web version of this article.)

2.4. Modifications to APSIM-Maize model and evaluation of impact

To evaluate the impact of the modified temperature response functions on simulated maize phenology and yield across the China Maize Belt under current climate and future warming scenarios, we replaced the original temperature functions for thermal time and RUE in the APSIM-Maize model with the newly derived temperature response functions. Both the original and modified models were calibrated and validated using data from the three sites where field data are available (Fig. 1). The validated models were then run against historical climate data (1961–2010) as well as warming scenarios by simply increasing the daily minimum and maximum temperatures together by +1, +2 and +3 °C. While real temperature changes exhibited asymmetrical patterns (e.g. night temperature increases more than daytime temperature), we used the simple change to evaluate the impact of likely inaccuracy in temperature response functions on simulated maize phenology and yield under non-stressed conditions (diseases and pest-free and no water and nitrogen stresses).

2.5. Statistical analysis

Root mean square error (RMSE) and normalized root mean square error (NRMSE) were used to evaluate the deviation between simulated and observed values:

$$RMSE = \sqrt{\frac{\sum_{i=1}^n (Y_i - X_i)^2}{n}} \quad (2)$$

$$NRMSE = \frac{RMSE}{\bar{X}} \times 100 \quad (3)$$

where X_i and Y_i are the observed and simulated phenology (days after sowing), biomass (kg/ha) and yield (kg/ha) respectively. \bar{X} is the mean of observed data.

3. Results

3.1. Comparison of temperature response functions

For temperature responses of leaf elongation rate, leaf appearance rate and the rate of development toward tasselling, flowering or silking, the data extracted from literatures are consistent with those measured

in the controlled-temperature environments for different maize cultivars (Fig. 1). The Wang-Engel function with $\beta = 1$ and three cardinal temperatures of 5 °C (T_b), 30 °C (T_o), and 41 °C (T_x) accurately describes the temperature responses for all the three processes overall (see statistical indices in Figs. 2 and 3). The derived optimal temperature of 30 °C is consistent with that of Parent and Tardieu (2012) (30 °C) and Yan and Hunt (1999) (31 °C), but lower than that used in the APSIM-Maize model (34 °C) and CERES-Maize model (> 40 °C). The derived base and maximum temperatures of 5 °C and 41 °C are consistent with Yan and Hunt (1999) (5 °C and 41 °C) but lower than those used in the APSIM-Maize model (8 °C and 44 °C) and CERES-Maize model (8 °C and no T_x), while they were not defined in Arrhenius-type curve used by Parent and Tardieu (2012).

In the controlled-temperature experiment, when maize exposed to high temperature (37.5 °C), Yunuo_7 (commonly adopted in Southwest China) had a much higher leaf appearance rate than other four maize cultivars adopted in Northeast China and North China Plain ($P < 0.05$, data not shown) while Nongda_386 (adopted in NCP) had a lower leaf elongation rate than other five cultivars ($P < 0.05$, data not shown). There were no significant differences in maize development rate during the vegetative growth period between the six cultivars ($P > 0.05$, data not shown).

The limited observed data on biomass growth or radiation use efficiency from the literatures could not permit the derivation of reliable temperature response function. However, APSIM and CERES used contrasting temperature response functions for RUE (Fig. 4). APSIM has a wider optimal temperature range (15–35 °C) and higher base and maximum temperatures, while CERES used a single optimal temperature (26 °C) with curvilinear response. Based on the data on temperature responses shown in Fig. 2, it was hard to imagine that the maximum temperature for RUE goes beyond 41 °C (the maximum temperature of organ development). In the absence of detailed data, we derived RUE response to temperature for maize using Wang-Engel function based on photosynthesis and respiration processes (Wang et al., 2017). Assuming the similar respiration process for C4 and C3 crop (Byrd et al., 1992), Wang-Engel function with $\beta = 0.8$, $T_b = 2$ °C, $T_o = 24$ °C and $T_x = 38$ °C was derived as the RUE curve response to temperature (Fig. 4).

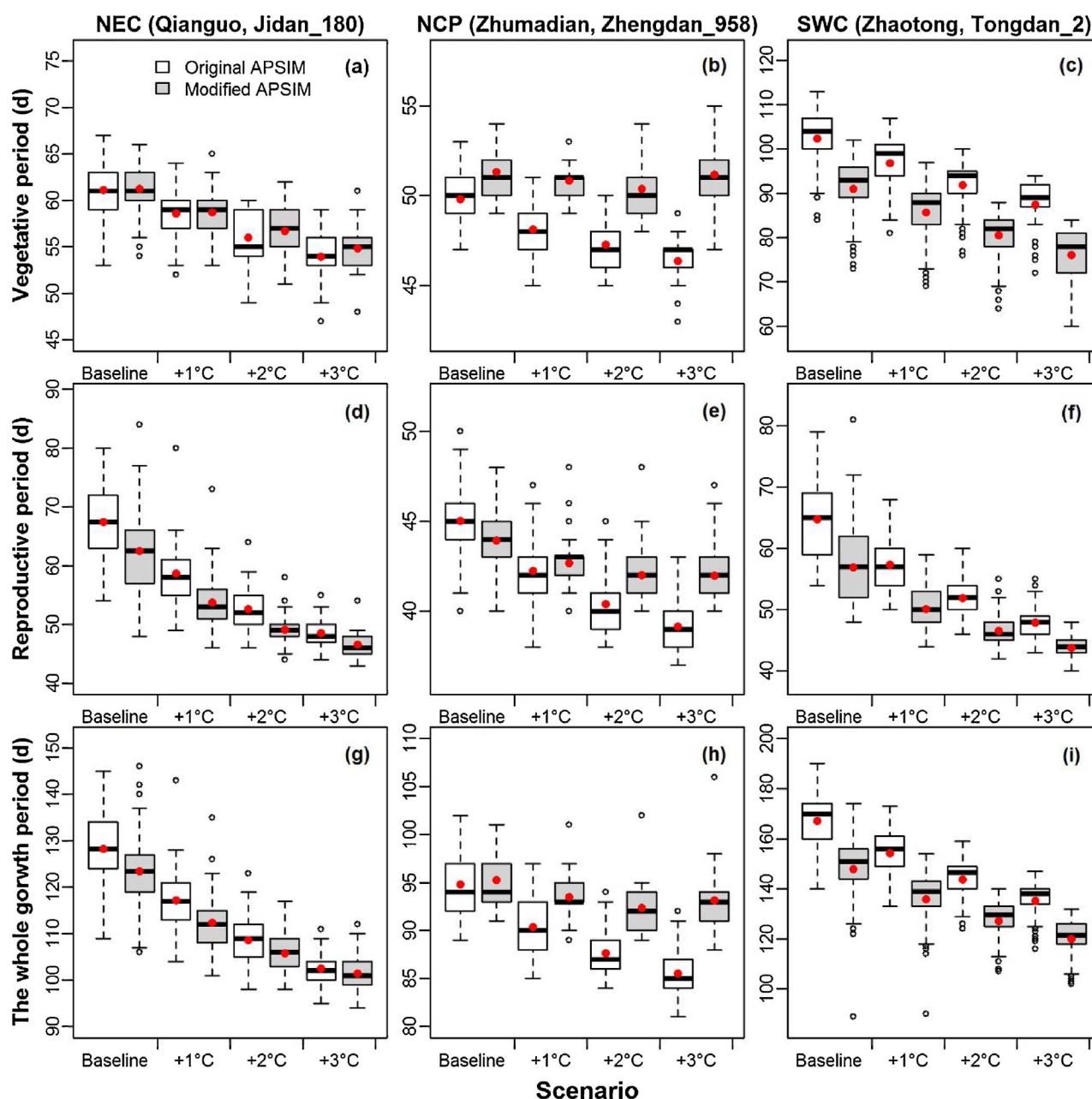


Fig. 6. Simulated duration from emergence to flowering (a–c), flowering to maturity (d–f) and emergence to maturity (g–i) by original and modified APSIM under baseline climate (1961–2010), +1 °C, +2 °C, +3 °C scenarios from the baseline in Northeast China (a, d, g), North China Plain (b, e, h) and Southwest China (c, f, i). Edges of box show 25% and 75% with the line and the solid circle within the box showing the median and the mean respectively. The whiskers extending to the most extreme data point are $1.5 \times (75-25\%)$ data range from the box.

3.2. Impact of temperature response functions on performance of APSIM model

APSIM-Maize model was modified by replacing the original temperature response functions for thermal time and RUE with the derived Wang-Engel functions in Figs. 2 and 4, respectively. Changes in the temperature response functions led to the need for re-calibration of the cultivar parameters at three maize growing regions of China (Table 3).

Calibration of both versions of APSIM models achieved similar performance (Fig. 5a–e). RMSE (NRMSE) between observed and simulated values by original and modified models were 2.2 d (18%) and 2.2 d (18%) for emergence date, 5.1 d (6.1%) and 6.0 d (7.2%) for flowering date, 6.8 d (4.9%) and 8.5 d (6.1%) for maturity date, respectively. For biomass and yield, original and modified APSIM have the similar RMSE (NRMSE), 3078 kg/ha (22.3%) and 3091 kg/ha (22.4%)

for biomass, 1340 kg/ha (19.4%) and 1319 kg/ha (19.1%) for yield, respectively.

Validation results showed that both the original and modified APSIM models can simulate independent datasets well after calibration (Fig. 5f–i). RMSE (NRMSE) between observed and simulated values by original and modified models were 0.33 d (3.3%) and 0.94 d (9.2%) for emergence date, 4.9 d (6.2%) and 4.9 d (6.2%) for flowering date, 7.4 d (5.5%) and 4.6 d (3.4%) for maturity date, respectively. For biomass and yield, original and modified APSIM have the similar RMSE (NRMSE), 2838 kg/ha (18.7%) and 3107 kg/ha (20.5%) for biomass, 944 kg/ha (13%) and 1291 kg/ha (17.7%) for yield, respectively.

3.3. Impacts on simulated phenology in response to temperature rise

Modification to the thermal time function impacted on the

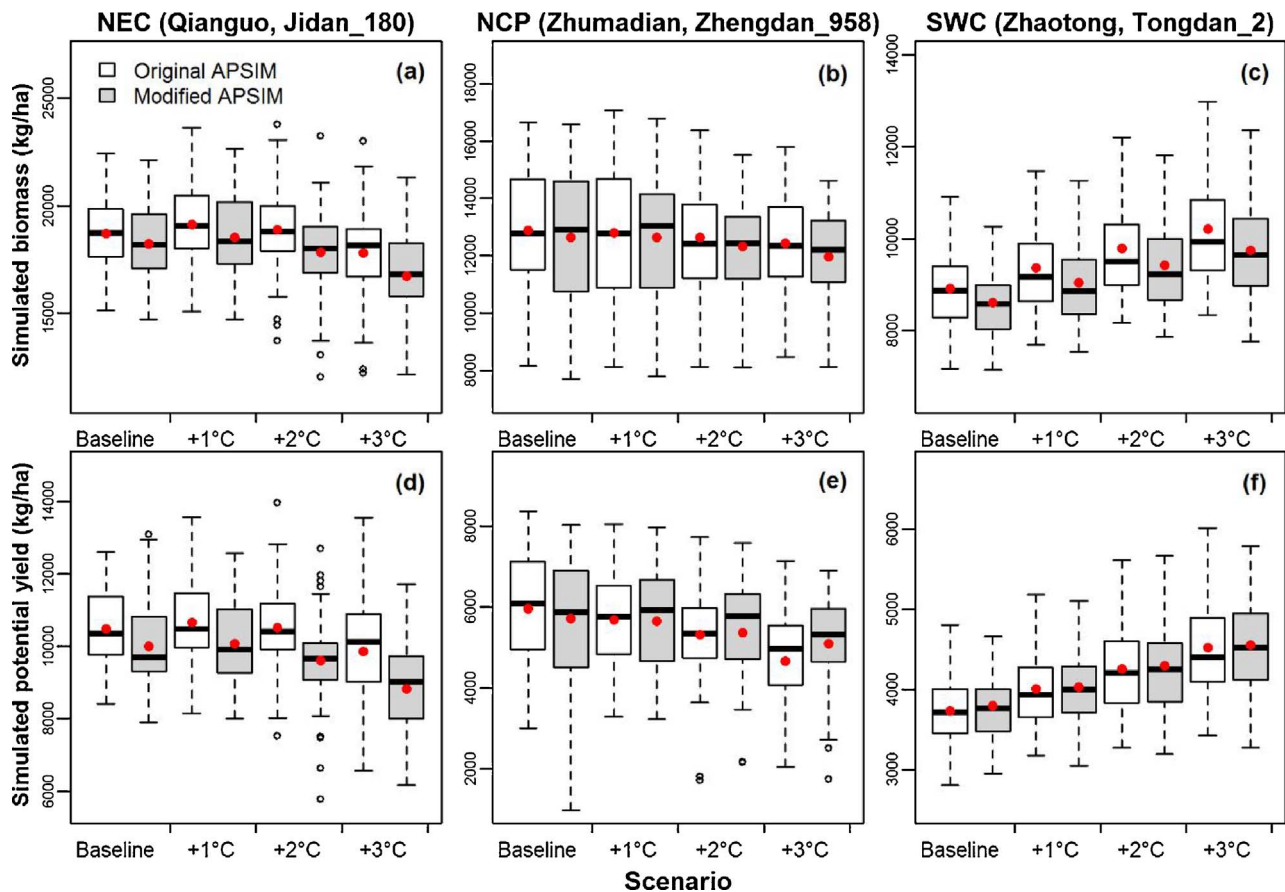


Fig. 7. Simulated biomass (a–c) and yield (d–f) by original and modified APSIM under baseline climate (1961–2010), +1 °C, +2 °C, +3 °C from the baseline scenarios in Northeast China (a, d), North China Plain (b, e) and Southwest China (c, f). Edges of box show 25% and 75% with the line and the solid circle within the box showing the median and the mean respectively. The whiskers extending to the most extreme data point are $1.5 \times (75-25\%)$ data range from the box.

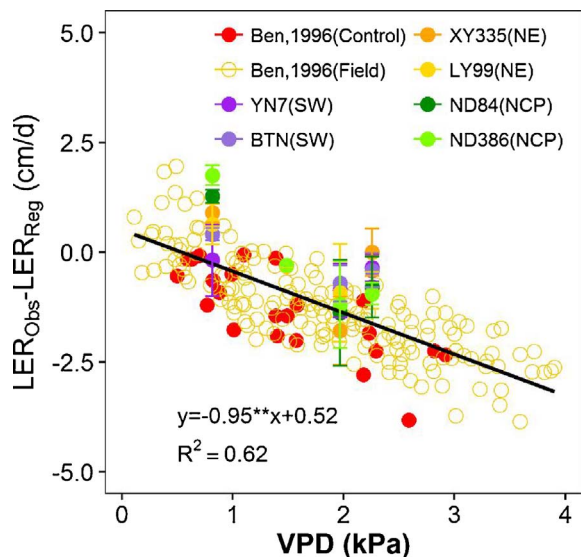


Fig. 8. The effect of vapour pressure deficit (VPD) on leaf elongation rate. $LER_{Obs} - LER_{Reg}$: difference between observed leaf elongations rates (LER_{Obs}) and estimated LER (LER_{Reg}) expected at the same air temperature, but low evaporative demand. LER_{Reg} is derived from the regression line with Wang-Engel function in Fig. 2a and air temperature.

simulated phenology of maize by APSIM (Fig. 6). For Northeast China, comparing to the original model and under the baseline climate, the modified model simulated a similar duration for vegetative phase (Fig. 6a), a shorter duration for reproductive period (Fig. 6d), and a consequently shorter total growth period (Fig. 6g). For North China

Plain, the modification led to a slightly longer vegetative duration (Fig. 6b), a shorter reproductive duration (Fig. 6e), and a similar total growth period as a result (Fig. 6h). For Southwest China, it simulated significantly reduced durations for all the growth periods (Fig. 6c, f, i).

Under temperature change scenarios of +1 ~ +3 °C, the modified model simulated shorter growth durations in NEC and SWC, but longer growth durations in NCP. Impact of modification to temperature functions on simulated phenology was the largest in NCP, and the least in NEC (Fig. 6).

3.4. Impact on simulated biomass and yield in response to temperature rise

While there were significant differences in simulated growth periods and their changes (in response to rising temperature) between original and modified APSIM, smaller differences were found in simulated biomass and yield and their changes between two models under the baseline and warming scenarios (Fig. 7). Due to significantly different growing season temperature, the trends in simulated biomass and yield with temperature rise varied between different sites. In NEC (Qianguo), simulated biomass and yield by two models would increase under +1 °C temperature scenario and then decrease with temperature rise (Fig. 7a, d). In NCP (Zhumadian), simulated biomass and yield by two models would decrease slightly under all the temperature rise scenarios (Fig. 7b, e). However, in SWC (Zhaotong), simulated biomass and yield by two models would increase under all the temperature rise scenarios (Fig. 7c, f). While both models simulated similar trends in response to temperature, the differences in simulated biomass and yield increased as temperature rise especially at warmer site.

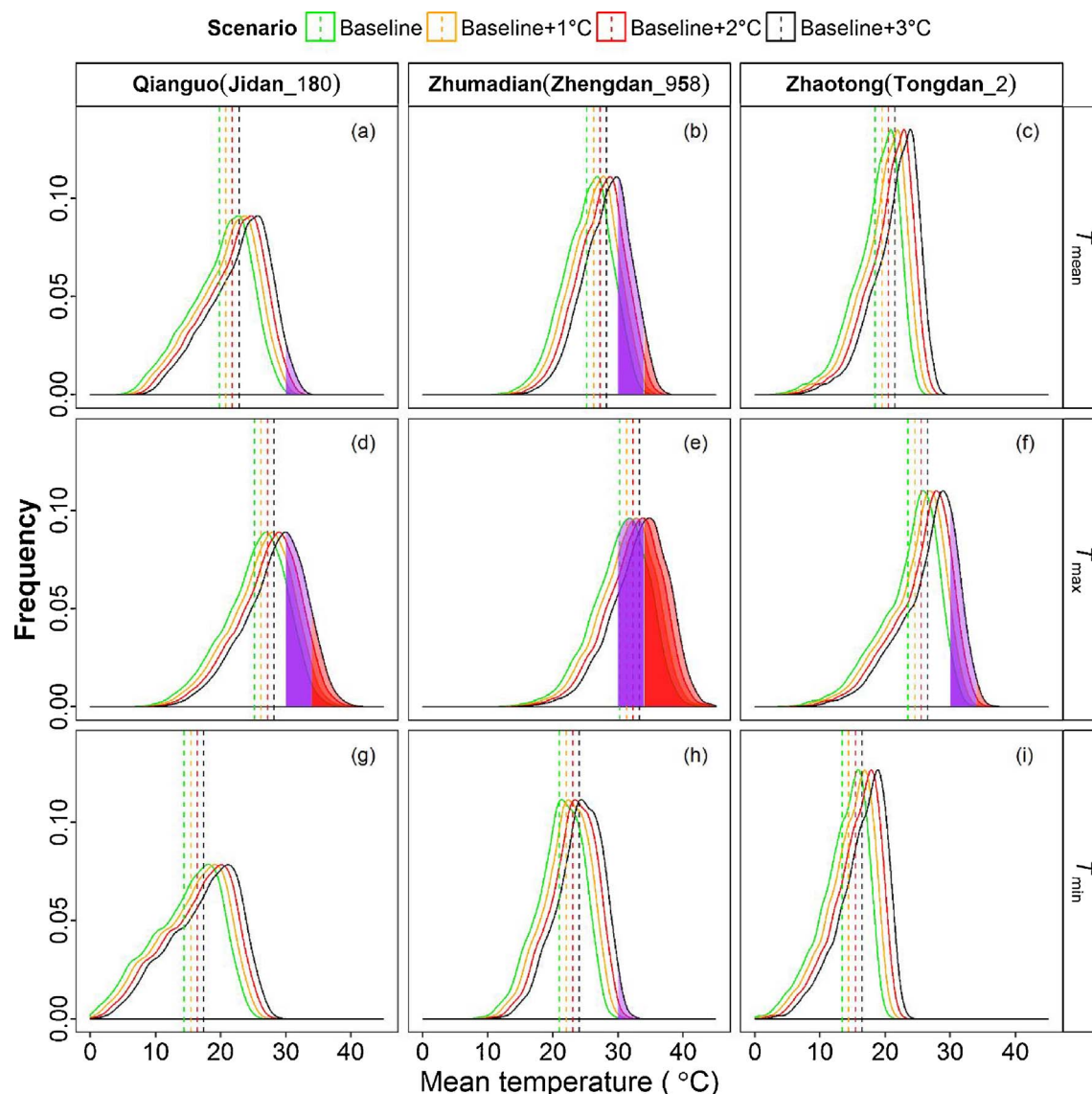


Fig. 9. Temperature distribution during maize growing season at three sites. Maize growing season is from May to September at Qianguo in NEC (a, d, g), from June to September at Zhumadian in NCP (b, e, h), from April to September at Zhaotong in SWC (c, f, i). Purple and red colour bands show temperature distribution in the range of 30–34 °C and > 34 °C, respectively. (For interpretation of the references to colour in this figure legend, the reader is referred to the web version of this article.)

4. Discussion

In this study, we combined data from literature and our controlled experiments to derive temperature response functions for phenological development and RUE of maize crop based on Wang-Engel function (Wang and Engel, 1998). For phenology, our derived base temperature (5 °C) was lower than what is used in APSIM (8 °C), possibly due to the use of a curvilinear relationship instead of a linear one. Our derived optimum and maximum temperatures (30 °C and 41 °C, respectively) are also lower than the default values in APSIM, but consistent with measurements (Fig. 2, Supplementary Fig. 1). Sanchez et al. (2014) also reviewed the studies on cardinal temperatures for maize growth and development and concluded that T_o varied in range of 29.2 ± 2.1 °C and T_x in range of 39.4 ± 2.0 °C, consistent with our findings.

The lower rates of leaf development derived based on the data from the controlled-temperature environment at high temperature of 37.5 °C may be subject to the impact of increase in vapour pressure deficit (VPD) (Fig. 2a). While a constant relative humidity (65%) was set in the phytotron, VPD increases with rising temperature. A negative effect of VPD on leaf elongation rate (LER) has been well documented

(Bouchabke et al., 2006; Salah and Tardieu, 1996) and increase in VPD also increases crop water demand, leading to more severe water stress (Wang et al., 2004). Our results matched the relationship between VPD and LER reported in the literature (Fig. 8). Previous controlled-temperature experiment studies set low VPD to minimize the interaction of VPD and temperature on leaf growth and development (Parent et al., 2010). Although VPD in the field could not reach such high value in the phytotron, the impact of VPD on leaf development rate should be considered in crop models for simulating crop growth and development in the environment of high air temperature and low air humidity. In our controlled experiment, almost all the maize plant died when exposed to 37.5 °C (day/night: 40/35 °C) in this study. Similar results were also found even for two cultivars from highland tropical when exposed to 37 °C (Ellis et al., 1992).

For the response of RUE to temperature, APSIM used an optimal temperature range of 15–35 °C, implying the same maximum RUE within the temperature range. However, Andrade et al. (1993) found RUE of maize increased with temperature from 16 °C to 21 °C. The maximum temperature of 50 °C in APSIM was also higher than the reported lethal temperature for maize plants in the field or controlled

environments ($46.0 \pm 2.9^\circ\text{C}$) (Sanchez et al., 2014). Our derived cardinal temperatures for RUE of maize are $T_b = 2^\circ\text{C}$, $T_o = 24^\circ\text{C}$ and $T_x = 38^\circ\text{C}$, which are more consistent with what the available data have shown. However, no reliable measurement data were found for RUE response to temperature above 26°C , implying that potential great uncertainty still exists.

In APSIM maize model, rate of phenological development is simulated using 3-hourly air temperatures interpolated from the daily maximum and minimum temperatures (Keating et al., 2003). Impact of diurnal variation in temperature is therefore accounted for. For RUE, APSIM uses daily mean temperature to modify RUE. The new temperature response for RUE here was derived with the method of Wang et al. (2017) to reflect the RUE response to daily mean temperature. The method derives the temperature response of RUE based on the temperature response of photosynthesis and respiration using a wide range of temperatures (daily maximum and minimum temperatures) and radiation conditions (Wang et al., 2017), thus implicitly considered the impact of diurnal variation in temperature and radiation.

Modification to the temperature functions of phenology and RUE caused significant differences in simulated maize growth stages and growth durations. These differences varied across regions in China due to the different temperature environments (seasonal distributions) in maize growing seasons (Fig. 9). Daily mean temperature (T_{mean}) during maize growing season increase from 19.9°C to 23.9°C at Qianguo (NEC, Fig. 9a) and from 17.7°C to 21.7°C at Zhaotong (SWC, Fig. 9c) as temperature increased from 0°C to $+3^\circ\text{C}$. In these two regions, the maize development rates almost linearly increased with seasonal temperature change, and the frequency of T_{mean} exceeded 30°C was relatively low. However, at Zhumadian in NCP, high T_{mean} , caused by high daily maximum and minimum temperatures (T_{max} and T_{min}) (Fig. 9e, h), increased from 25.2°C to 28.2°C as under base ($+0^\circ\text{C}$) and temperature rising scenarios (up to $+3^\circ\text{C}$) (Fig. 9b). Frequency of T_{mean} exceeded 30°C increased significantly (Fig. 9b), leading to contrasting simulated phenology between original and modified APSIM, especially in the temperature range of $30\text{--}34^\circ\text{C}$ (Fig. 2d).

In general, shortened growth period led to the decline in potential (Guereña et al., 2001; Tao et al., 2006; Wang et al., 2012, 2014), which was the case at Zhumadian under $+1^\circ\text{C}$ and $+2^\circ\text{C}$ temperature scenarios and at Qianguo under all warming scenarios. However, at cooler site (Zhaotong), temperature rise would lead to the increase in simulated potential yield because the positive contribution of increasing RUE on maize yield offset the negative contribution of shortened growing period on yield (Supplementary Table S2). Moreover, at Zhumadian, when temperature increased by $+3^\circ\text{C}$, prolonged growth period failed to increase maize potential yield because of the significant negative influence of high temperature on daily RUE (Supplementary Table S2). Although the modification to temperature functions had less impact on simulated final maize yield (as compared to the original model), the modified model simulated different interactions between phenological changes, biomass growth and yield formation, implying potential genotype by environmental interactions.

Acknowledgements

This work is supported by the National Key Research and Development Program of China (2017YFD0300304), National Agricultural Introducing Intelligence Platform (2015z007) and China Scholarship Council under the CSIRO-Chinese Ministry of Education (MoE) PhD Fellowship Research Program. We would like to thank China Meteorological Administration for providing the historical climate data.

Appendix A. Supplementary data

Supplementary material related to this article can be found, in the online version, at doi:<https://doi.org/10.1016/j.agrformet.2018.01>.

005

References

- Andrade, F.H., Uhart, S.A., Cirilo, A., 1993. Temperature affects radiation use efficiency in maize. *Field Crops Res.* 32 (1–2), 17–25.
- Asseng, S., et al., 2013. Uncertainty in simulating wheat yields under climate change. *Nat. Clim. Change* 3 (9), 827–832.
- Badu, A.B., Hunter, R., Tollenaar, M., 1983. Effect of temperature during grain filling on whole plant and grain yield in maize (*Zea mays* L.). *Can. J. Plant Sci.* 63 (2), 357–363.
- Bassu, S., et al., 2014. How do various maize crop models vary in their responses to climate change factors? *Global Change Biol.* 20 (7), 2301–2320.
- Bouchabke, O., Tardieu, F., Simonneau, T., 2006. Leaf growth and turgor in growing cells of maize (*Zea mays* L.) respond to evaporative demand under moderate irrigation but not in water-saturated soil. *Plant Cell Environ.* 29 (6), 1138–1148.
- Brown, D., Bootsma, A., 1993. Crop heat units for corn and other warm-season crops in Ontario. *Factsheet. Agdex/Ont. Min. Agric. Food* 111, 31.
- Byrd, G.T., Sage, R.F., Brown, R.H., 1992. A comparison of dark respiration between C3 and C4 plants. *Plant Physiol.* 100 (1), 191–198.
- Ellis, R., Summerfield, R., Edmeades, G., Roberts, E., 1992. Photoperiod, temperature, and the interval from sowing to tassel initiation in diverse cultivars of maize. *Crop Sci.* 32 (5), 1225–1232.
- FAO, 2014. <http://faostat3.fao.org/download/Q/QC/E>.
- Fleisher, D.H., et al., 2017. A potato model intercomparison across varying climates and productivity levels. *Global Change Biol.* 23 (3), 1258–1281.
- Gilmore, E., Rogers, J., 1958. Heat units as a method of measuring maturity in corn. *Agron. J.* 50 (10), 611–615.
- Guereña, A., Ruiz-Ramos, M., Díaz-Ambrona, C.H., Conde, J.R., Mínguez, M.I., 2001. Assessment of climate change and agriculture in Spain using climate models. *Agron. J.* 93 (1), 237–249.
- Hunter, R., Tollenaar, M., Breuer, C., 1977. Effects of photoperiod and temperature on vegetative and reproductive growth of a maize (*Zea mays*) hybrid. *Can. J. Plant Sci.* 57 (4), 1127–1133.
- IPCC, 2012. Managing the risks of extreme events and disasters to advance climate change adaptation. In: Field, C.B., Barros, V., Stocker, T.F., Qin, D., Dokken, D.J., Ebi, K.L., Mastrandrea, M.D., Mach, K.J., Plattner, G.-K., Allen, S.K., Tignor, M., Midgley, P.M. (Eds.), *A Special Report of Working Groups I and II of the Intergovernmental Panel on Climate Change*. Cambridge University Press, Cambridge, UK, and New York, NY, USA 582 pp.
- IPCC, 2014. Climate change 2014: impacts, adaptation, and vulnerability part B: regional aspects. In: Barros, V.R., Field, C.B., Dokken, D.J., Mastrandrea, M.D., Mach, K.J., Bilir, T.E., Chatterjee, M., Ebi, K.L., Estrada, Y.O., Genova, R.C., Girma, B., Kissel, E.S., Levy, A.N., MacCracken, S., Mastrandrea, P.R., White, L.L. (Eds.), *Contribution of Working Group II to the Fifth Assessment Report of the Intergovernmental Panel on Climate Change*. Cambridge University Press, Cambridge, UK and New York, NY, USA, pp. 1327–1370.
- Jones, C.A., Kiniry, J.R., 1986. *CERES-Maize: A Simulation Model of Maize Growth and Development*. Texas A&M University Press.
- Keating, B.A., et al., 2003. An overview of APSIM, a model designed for farming systems simulation. *Eur. J. Agron.* 18 (3), 267–288.
- Kiesselbach, T.A., 1950. Progressive development and seasonal variations of the corn crop. *Neb. Agric. Exp. Stn. Res. Bull.* 166.
- Li, T., et al., 2015. Uncertainties in predicting rice yield by current crop models under a wide range of climatic conditions. *Global Change Biol.* 21 (3), 1328–1341.
- Liu, Z., Yang, X., Hubbard, K.G., Lin, X., 2012. Maize potential yields and yield gaps in the changing climate of northeast China. *Global Change Biol.* 18 (11), 3441–3454.
- Lobell, D.B., et al., 2013. The critical role of extreme heat for maize production in the United States. *Nat. Clim. Change* 3 (5), 497–501.
- Lobell, D.B., Schlenker, W., Costa-Roberts, J., 2011. Climate trends and global crop production since 1980. *Science* 333 (6042), 616–620.
- Parent, B., Tardieu, F., 2012. Temperature responses of developmental processes have not been affected by breeding in different ecological areas for 17 crop species. *New Phytol.* 194 (3), 760–774.
- Parent, B., Tardieu, F., 2014. Can current crop models be used in the phenotyping era for predicting the genetic variability of yield of plants subjected to drought or high temperature? *J. Exp. Bot.* 65 (21), 6179–6189.
- Parent, B., Turc, O., Gibon, Y., Stitt, M., Tardieu, F., 2010. Modelling temperature-compensated physiological rates, based on the co-ordination of responses to temperature of developmental processes. *J. Exp. Bot.* 61 (8), 2057–2069.
- Parry, M.L., Rosenzweig, C., Iglesias, A., Livermore, M., Fischer, G., 2004. Effects of climate change on global food production under SRES emissions and socio-economic scenarios. *Global Environ. Change* 14 (1), 53–67.
- Piao, S., et al., 2010. The impacts of climate change on water resources and agriculture in China. *Nature* 467 (7311), 43–51.
- Rosenzweig, C., Wilbanks, T.J., 2010. The state of climate change vulnerability, impacts, and adaptation research: strengthening knowledge base and community. *Clim. Change* 100 (1), 103–106.
- Salah, H.B.H., Tardieu, F., 1996. Quantitative analysis of the combined effects of temperature, evaporative demand and light on leaf elongation rate in well-watered field and laboratory-grown maize plants. *J. Exp. Bot.* 47 (11), 1689–1698.
- Sanchez, B., Rasmussen, A., Porter, J.R., 2014. Temperatures and the growth and development of maize and rice: a review. *Global Change Biol.* 20 (2), 408–417.
- Siebert, S., Ewert, F., Rezaei, E.E., Kage, H., Graß, R., 2014. Impact of heat stress on crop yield-on the importance of considering canopy temperature. *Environ. Res. Lett.* 9 (4), 044012.

- Stewart, D.W., Dwyer, L.M., Carrigan, L.L., 1998. Phenological temperature response of maize. *Agron. J.* 90 (1), 73–79.
- Tao, F., Yokozawa, M., Xu, Y., Hayashi, Y., Zhang, Z., 2006. Climate changes and trends in phenology and yields of field crops in China, 1981–2000. *Agric. Forest Meteorol.* 138 (1–4), 82–92.
- Tao, F., Zhang, Z., 2010. Adaptation of maize production to climate change in North China Plain: quantify the relative contributions of adaptation options. *Eur. J. Agron.* 33 (2), 103–116.
- Wang, E., Engel, T., 1998. Simulation of phenological development of wheat crops. *Agric. Syst.* 58 (1), 1–24.
- Wang, E., Engel, T., 2000. SPASS: a generic process-oriented crop model with versatile windows interfaces. *Environ. Modell. Softw.* 15 (2), 179–188.
- Wang, E., et al., 2017. The uncertainty of crop yield projections is reduced by improved temperature response functions. *Nat. Plants* 3, 17102.
- Wang, E., Smith, C.J., Bond, W.J., Verburg, K., 2004. Estimations of vapour pressure deficit and crop water demand in APSIM and their implications for prediction of crop yield, water use, and deep drainage. *Aust. J. Agric. Res.* 55 (12), 1227–1240.
- Wang, J., Wang, E., Yang, X., Zhang, F., Yin, H., 2012. Increased yield potential of wheat-maize cropping system in the North China Plain by climate change adaptation. *Clim. Change* 113 (3–4), 825–840.
- Wang, J., Wang, E., Yin, H., Feng, L., Zhang, J., 2014. Declining yield potential and shrinking yield gaps of maize in the North China Plain. *Agric. Forest Meteorol.* 195–196, 89–101.
- Wang, J., Wang, E.L., Liu, D.L., 2011. Modelling the impacts of climate change on wheat yield and field water balance over the Murray-Darling Basin in Australia. *Theor. Appl. Climatol.* 104 (3–4), 285–300.
- Wang, N., et al., 2015. Increased uncertainty in simulated maize phenology with more frequent supra-optimal temperature under climate warming. *Eur. J. Agron.* 71, 19–33.
- Warrington, I., Kanemasu, E., 1983. Corn growth response to temperature and photoperiod I. Seedling emergence, tassel initiation, and anthesis. *Agron. J.* 75 (5), 749–754.
- Xiong, W., et al., 2009. Future cereal production in China: the interaction of climate change, water availability and socio-economic scenarios. *Global Environ. Change* 19 (1), 34–44.
- Yan, W., Hunt, L., 1999. An equation for modelling the temperature response of plants using only the cardinal temperatures. *Ann. Bot.* 84 (5), 607–614.
- Yin, X., Kropff, M.J., McLaren, G., Visperas, R.M., 1995. A nonlinear model for crop development as a function of temperature. *Agric. Forest Meteorol.* 77 (1), 1–16.